Heat and Mass Transfer
https://doi.org/10.1007/s00231-023-03384-6

ORIGINAL ARTICLE

Role of zinc in bulk precipitation from the steaming process of potable water

Amthal Al-Gailani[1] · Martin J. Taylor[1] · Richard Barker[2]

Received: 18 April 2023 / Accepted: 14 June 2023

Abstract
Water chemistry plays an important role in fouling kinetics and morphology. This work investigates the influence of zinc cations in potable water, specifically the kinetics of crystallisation and their effect on the fouling layer during the operation of a batch steam generator system and a once-through flow system. The kinetics of precipitation in the batch crystalliser were examined based on the change in concentration of the foulants, while the fouling resistance approach was used in the flow system. In addition, morphological testing was carried out using Scanning Electron Microscopy, Powder X-ray Diffraction, and Energy dispersive X-ray. The findings showed that the precipitation rate of calcium carbonate decreases with the increase in zinc ions until reaching the zinc carbonate supersaturation in the water due to water evaporation. Regarding morphology, co-precipitation of zinc carbonate was observed at high zinc concentrations. As a result, a double effect was observed where zinc both retarded and enhanced fouling over time. The fouling rate in the flow system decreased as the zinc concentration increased. Zinc ions were found to influence the morphology of deposit minerals significantly. Moreover, the surface deposition of zinc salts increased with the solution content of zinc.

1 Introduction

The presence of simple metal ions or complex ions in water may pose an inhibitory impact on the nucleation and growth process of mineral scale crystals. Scale is the formation of unwanted solid minerals onto the heat transfer surfaces and bulk solutions, for example, inside the piping system, in valves, heat exchangers etc. In household appliances, a composite scale of different minerals ($CaCO_3$, $MgCO_3$ and $CaSO_4$) might form due to the presence of a variety of ionic species in potable water. Therefore, understanding surface deposition and bulk precipitation from potable water in domestic appliances is a real challenge for consumers and manufacturers.

At low concentrations, cationic additives like magnesium, copper, zinc, lead, manganese, nickel, and iron could adsorb onto the active growth positions on the precipitate particles [1]. Zinc is present in potable and surface water at a concentration of up to 15 mg/L. The primary sources of zinc in potable and surface water are leached or discharged from steel production by-products (slag) or coal-fired power station waste [2].

Water treatment devices use a scale reducer made of elemental zinc, which may corrode, releasing zinc cations (Zn^{2+}) into the water. For almost the first time, Coetzee and Howell [3] reported the inhibitory impact of zinc on scale formation. They use three types of physical water treatment methods with low concentrations of Zn^{2+}. The inhibitory effect of zinc ions on the bulk precipitation of scale particles has been reported in a few other studies, such as Zachara, et al. [4], who emphasised rapid adsorption of Zn^{2+} on calcite (hexagonal calcium carbonate) according to the exchange of Zn^{2+} and $ZnOH^+$ with surface-bonded Ca^{2+}. However, it has also been confirmed that Zn can react with carbonate ions, forming $ZnCO_3$ crystals that enhance heterogeneous nucleation [5, 6].

In some household devices, steaming is typical, leading to unavoidable mineral scaling from potable water. However, the role of zinc in the crystallisation fouling of inorganic minerals during a steaming process or water boiling has received inadequate attention. During a steaming process, the supersaturation of different inversely soluble

✉ Amthal Al-Gailani
A.Z.Al-Gailani@hull.ac.uk

[1] Department of Chemical Engineering, School of Engineering, University of Hull, Hull HU6 7RX, United Kingdom

[2] School of Mechanical Engineering, University of Leeds, Leeds LS2 9JT, United Kingdom

Published online: 03 July 2023

minerals is affected by both temperature change and the evaporation of water.

In this work, the effects of zinc ions on the crystallisation fouling in the bulk solution and the heated surface from potable water were investigated during the steaming process using two unique experimental setups to mimic different household appliances. A batch configuration can be seen in kitchen kettles and small boilers, while the flow system is dominant among household devices such as central heating.

Varying concentrations of Zn^{2+} were used (0 to 15 mg/L) to examine the impact on the fouling kinetics and scale particle morphology during the steaming process in both setups. The bulk crystallisation of the zinc minerals was studied using spectroscopic analysis. The surface deposition was examined on an aluminium surface using a fouling resistance approach and deposits mass.

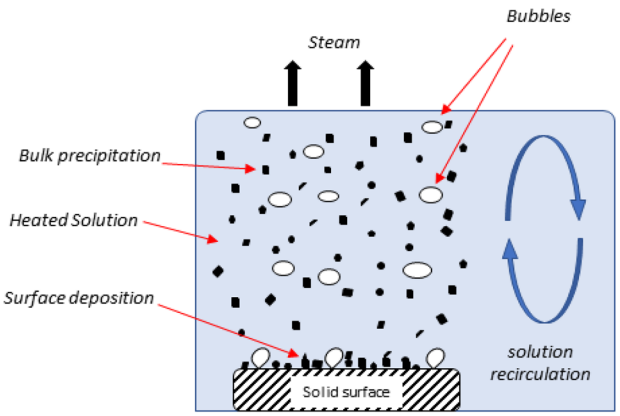

Fig. 1 Representation of bulk precipitation in the experimental vessel

2 Materials and methods

2.1 Batch crystalliser system

The first part of the experiments was conducted using a batch crystalliser in which the precipitated scale particles in the bulk fluid and solid surface can be evaluated, as shown in Fig. 1. The solution's turbidity and ionic zinc concentration were quantitatively measured for bulk precipitation kinetics. In addition, the solution content of Zn^{2+} was measured as a function of time, following a proper sampling procedure. Also, as the heat was constantly supplied, the bulk temperature increased with time. As a result, the solution supersaturation, with respect to mineral salts, was reduced with time in such a closed system. This unique setup was developed to mimic a batch evaporation process in domestic and industrial systems.

The setup consists of a 1000 mL borosilicate glass beaker, hot plate (Heidolph), Pt1000 thermocouple (ThermoScientific), and metallic samples. The test specimen was constructed of stainless steel 316L (SS31603) for minimising the potential of corrosion product formation.

2.2 Once-through flow system

In this setup, the inorganic fouling of the heat transfer surface associated with partial water evaporation was studied during pool boiling. This setup was an open system where a once-through flow was adopted. Figure 2 illustrates the schematic of surface deposition under the conditions used in the present experiments. The schematic diagram of the experimental apparatus is shown in Fig. 3. It consists of a solution tank, peristaltic pump, test flow cell, sample heating system, data acquisition system and waste tank. This

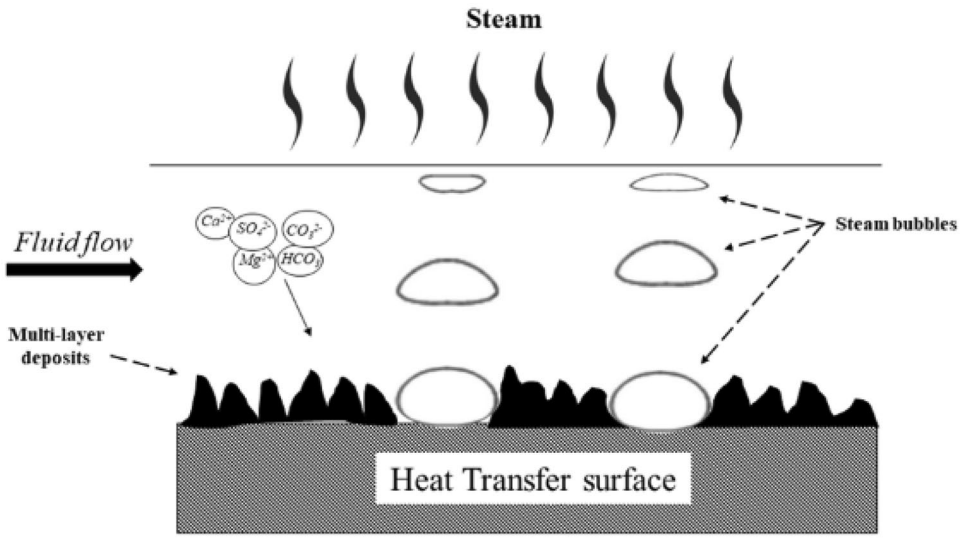

Fig. 2 Schematic of surface deposition in the once-through flow system

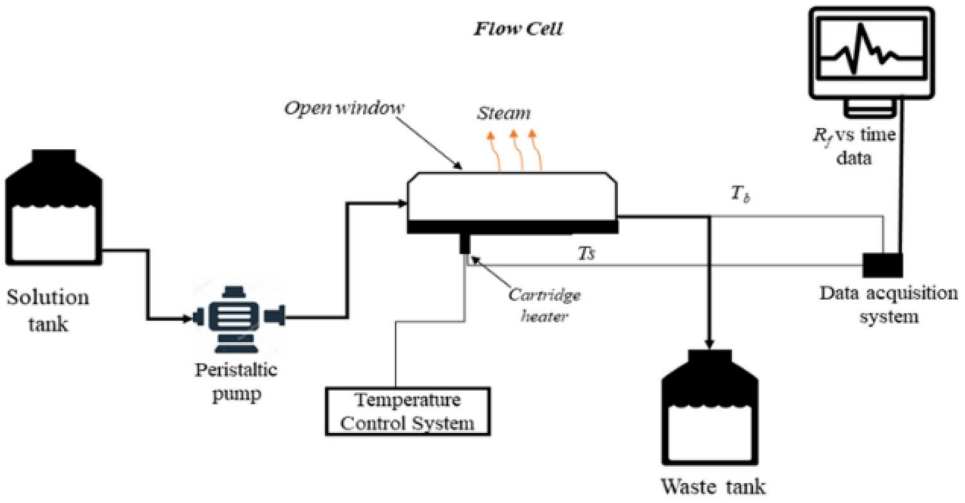

Fig. 3 Configuration of the once-through flow system

once-through flow system was adopted to avoid any reduction in the saturation state, which may result from solution re-circulation.

Aluminium alloy 1050A (Al ≥ 99.5%) was used to fabricate the test specimen, which was chosen as it is one of the most common materials used in constructing heat transfer surfaces in household appliances. The influence of the resistive fouling layer on the heat transfer was evaluated using fouling resistance. The design details of the test flow cell, dimensions of test specimens, method of the fouling resistance calculation, data acquisition system and the experimental procedure are reported in our previous work Al-Gailani, et al. [7].

The flow cell was designed to obtain a fully developed laminar flow on the tested aluminium surface at an average 8 mL/min flow rate. The surface temperature was maintained At a constant 100 °C under atmospheric pressure. The test specimen surface was ground with silicon carbide paper (1200 grit) and then polished with a diamond suspension (0.5 µm) to obtain an arithmetical mean roughness of 22.4 – 31.2 nm.

2.3 Test solutions

The base test solution used in both systems is commercially-available bottled water (Evian® Natural Spring Water) with a pH of 7.2. It has been chosen for its hardness due to 307 ppm of $CaCO_3$, which is almost the same as potable water hardness in some areas of the south of the United Kingdom. The composition of the base solution is listed in Table 1. The main test solutions were prepared by adding Zinc sulphate monohydrate $ZnSO_4.H_2O$ (Sigma Aldrich, Min. 99.9%) to the base solution to produce solutions of 5, 10, and 15 mg/L of zinc.

For the crystallisation fouling in the batch system, 1 mL of the test solution was taken from the test vessel at specific time intervals. The solution volume was mixed with a 9 mL quenching (KCl/polyvinyl sulfonate) solution to prevent further precipitation [8].

Table 1 Composition of the base solution

Ionic species	mg/L
Ca^{2+}	80.0
Mg^{2+}	26.0
Na^{+}	6.5
K^{+}	1.0
Si^{4+}	15.0
HCO^{3-}	360.0
SO_4^{2-}	14.0
Cl^{-}	10.0
NO^{3-}	3.8
Dry residue at 180ºC	345.0

2.4 Surface and solution characterisation

At the end of the experiment, the weight of the metallic sample was evaluated, and the surface deposits were characterised. While the 10 mL solution samples were used to assess the bulk concentration of cations (Ca, Zn, Na, Mg, K and Si) by Flame Atomic Absorption Spectrophotometer (AAS) (Agilent Technologies, Model: 240FS AA, USA). Besides the AAS samples, an aliquot of 10 mL was taken at the same time intervals for the turbidity measurements conducted using a DR-890 Colorimeter (CAMLAB). The deposit morphology was examined using a Philips X'Pert X-ray diffractometer (PXRD) (X'Pert MPD, Cu anode x-ray source, Netherlands) and a Carl Zeiss EVO MA15 Scanning Electron Microscope. Samples were coated with iridium (Ir) at a thickness of 10 nm using sputter coating to avoid charge build-up on a sample surface. Energy dispersive

X-ray (EDX) elemental analysis was used to determine the composition of scale particles.

3 Results and discussion

3.1 Fouling crystallisation in the batch system

The effect of Zn^{2+} on the bulk crystallisation of inorganic minerals from potable water was studied. Figure 4a displays the profile of Ca^{2+} concentration during the heating of the zinc-containing potable water from room temperature to boiling under atmospheric pressure. In the zinc-free solution, the content of Ca^{2+} decreases at a temperature of ~57 °C after 5 min of heating. The time taken for Ca^{2+} (induction time) to reduce is prolonged as the Zn^{2+} content increases. On the contrary, the concentration of Ca^{2+} increases to a maximum point due to water evaporation with temperature increase. This maximum point in the Ca^{2+} concentration profile represents the supersaturation of $CaCO_3$ with respect to temperature and solution volume. However, it decreases when attaining the required supersaturation for the scale to precipitate. The Zn^{2+} in solution complexes with the carbonate fouling species increases the energy barrier of the crystallisation reaction [9–11]. It has been reported that zinc may react with CO^{3-} resulting in the formation of stable $ZnCO_3$, competing with Ca^{2+} [5].

The sharp reduction in the Ca^{2+} concentration for cases with Zn^{2+} indicates that zinc inhibition has ended. The AAS analysis in Fig. 4b shows that Zn^{2+} concentration in the solution decreases with temperature and time. It is expected that the Zn^{2+} to increase due to the evaporation of water as the temperature increases. The zinc ions are involved in reactions with the fouling species for the formation of zinc minerals or inhibiting precipitation of other minerals. Forming a complex with HCO^{3-}, CO^{3-} and Ca^{2+} might be the case in the first period of heating (<85 °C) [9]. However, for steeper depletion in Zn^{2+} (>85 °C), the crystallisation of $ZnCO_3$ occurs [12].

The results of the Ca^{2+} profile at different zinc concentrations were interpreted into the crystallisation induction time, as shown in Fig. 5a. The time it takes for the first visible crystal to appear in the bulk solution, the induction time, increases exponentially with an increase in zinc content in the water. This confirms that zinc forms a complex with the fouling species during the initial heating period, preventing the crystallisation reaction [13].

Figure 5b illustrates the solution turbidity as a function of time for various concentrations of Zn^{2+}. The solution turbidity increases with time for all solutions. However, the turbidity of the high Zn^{2+} solutions (10 and 15 mg/L) is the lowest at the later stages of heating. The turbidity measurement indicates the solution cloudiness caused by the suspended

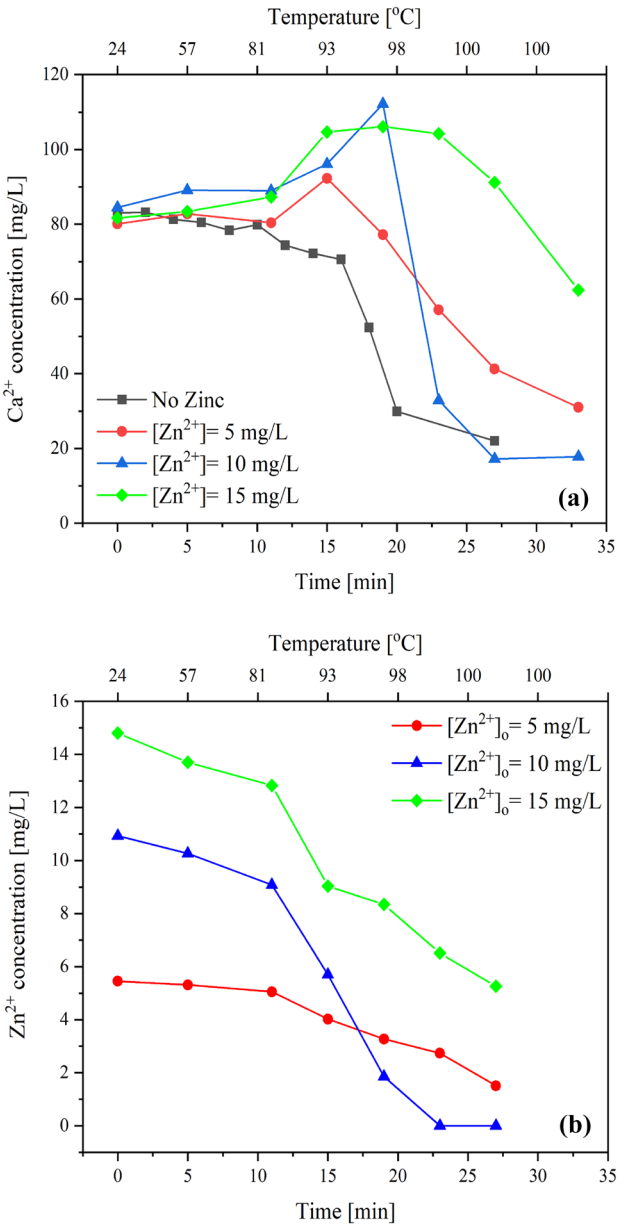

Fig. 4 (**a**) Ca^{2+} concentration profile and (**b**) Zn^{2+} concentration profile, during water heating for different $ZnSO_4$ concentrations

scale particles. As the density of the $ZnCO_3$ is 2x that of $CaCO_3$, the $ZnCO_3$ crystals tend to precipitate faster than $CaCO_3$ or $MgCO_3$ [14], resulting in less turbidity.

The effect of Zn^{2+} on the scale morphology is presented in SEM and PXRD analysis in Figs. 6a, b and 7. The SEM observations in Fig. 6 show that the deposits with no zinc mainly comprise needle-like aragonite (Orthorhombic $CaCO_3$). However, at 15 mg/L, mineral deposits transform into lumpy crystals, which are attributed to the precipitation of $ZnCO_3$. The presence of $ZnCO_3$ as smithsonite was confirmed by PXRD analysis, as shown in Fig. 7. A small peak corresponding to ZnO is also observed.

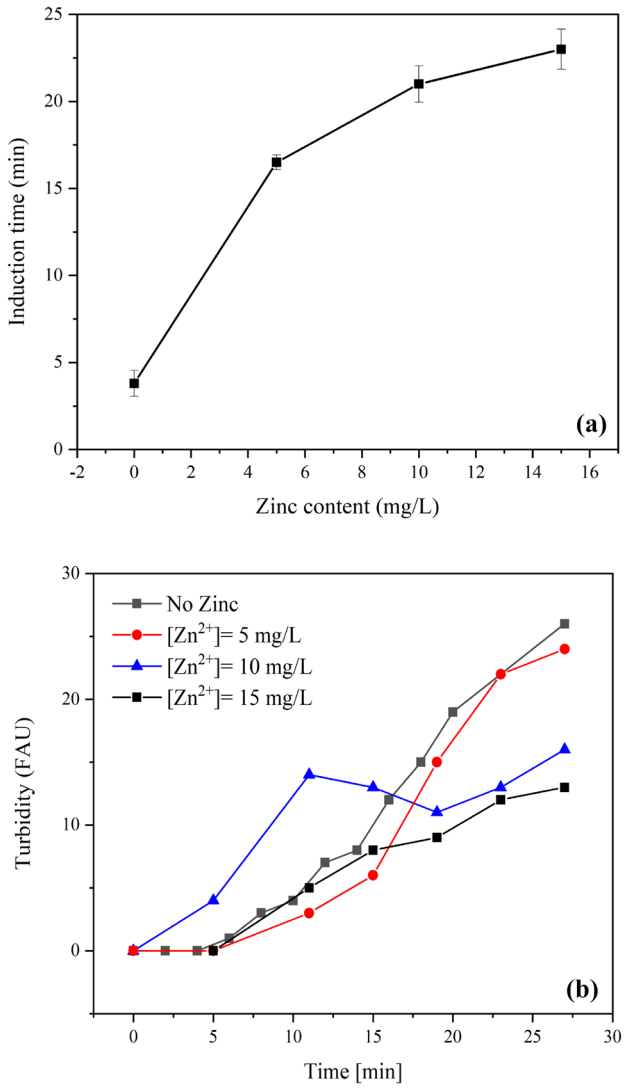

Fig. 5 (**a**) Crystallisation induction time and (**b**) solution turbidity for different Zn concentrations

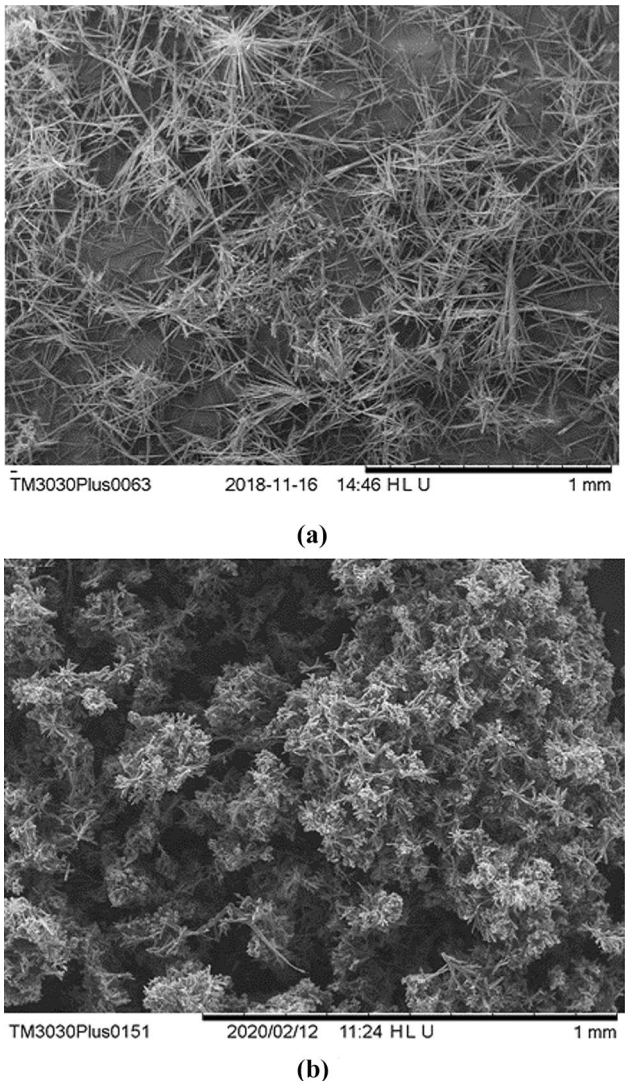

Fig. 6 SEM images of (**a**) the precipitated scale with no Zn in water and (**b**) with 15 mg/L Zn^{2+}

At high concentrations, Zn^{2+} interacts with HCO^{3-} or CO^{3-} to form zinc inversely soluble salts such as $[Zn(CO_3)_2]^{2-}$, $Zn_5(CO_3)_2(OH)_6$ and $ZnCO_3$ [6]. These minerals co-precipitate with other minerals such as $CaCO_3$ and $MgCO_3$. Some minerals like $[Zn(CO_3)_2]^{2-}$ are more likely to act as a site for other mineral nucleation and growth. The precipitation of zinc minerals retards the heat transfer as it adds more insulation to the surface.

3.2 Fouling crystallisation in the once-through flow system

The effect of the free zinc ion has been investigated on the composite crystallisation fouling from potable water. The findings show that the thermal fouling resistance drops as the concentration of Zn^{2+}, as shown in Fig. 8a. It also illustrates that Zn^{2+} concentration can also affect the induction time. For example, the asymptotic fouling resistance was reduced by half when the Zn^{2+} concentration increased by 15 mg/L (Fig. 8b). The exponential decay of asymptotic fouling resistance refers to the decreasing inhibition efficiency of zinc. For example, it has been reported that Zn2+ inhibits the nucleation of CaCO3 with a concentration starting from 0.02 mg/L [15]. For the same range, the mass of deposits decreased by 25.3 mg.

Figure 9a shows an exponential growth relationship between the asymptotic fouling resistance and the scale mass. However, this relationship may indicate variation in the physical properties of the fouling crust, such as density, thermal conductivity and porosity. As mentioned earlier, the Zn^{2+} exhibits a pronounced impact on the induction period. The scaling induction time increased from 78

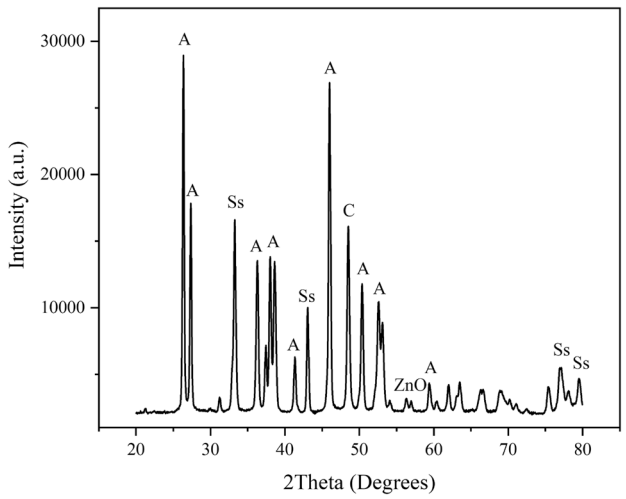

Fig. 7 XRD diffractogram of bulk precipitate in the presence of 15 mg/L zinc (A: aragonite, C: calcite, and Ss: Smithsonite)

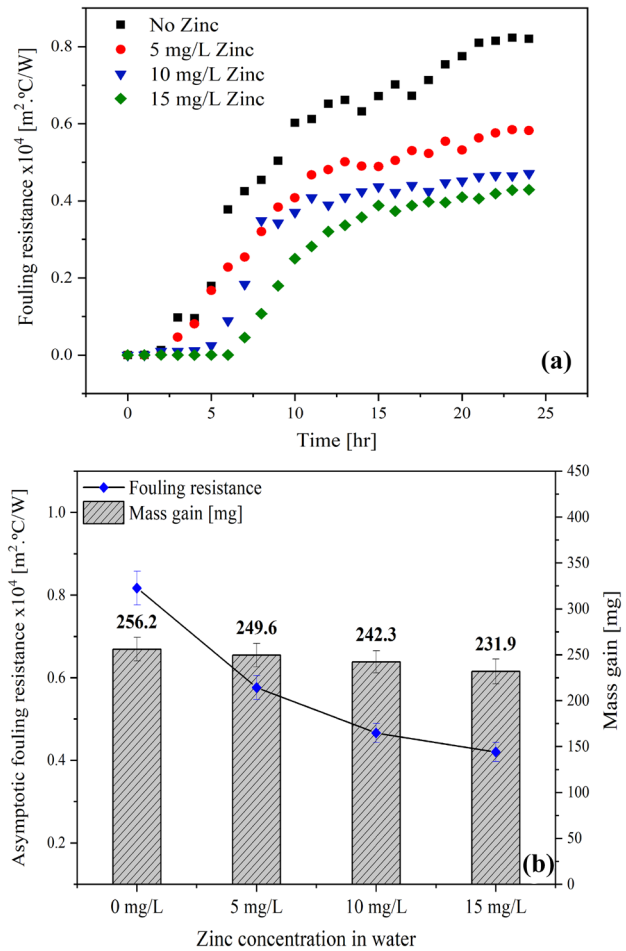

Fig. 8 (**a**) Thermal fouling resistance of scale on the aluminium surface and (**b**) surface mass gain and asymptotic fouling resistance for different contents of zinc in water

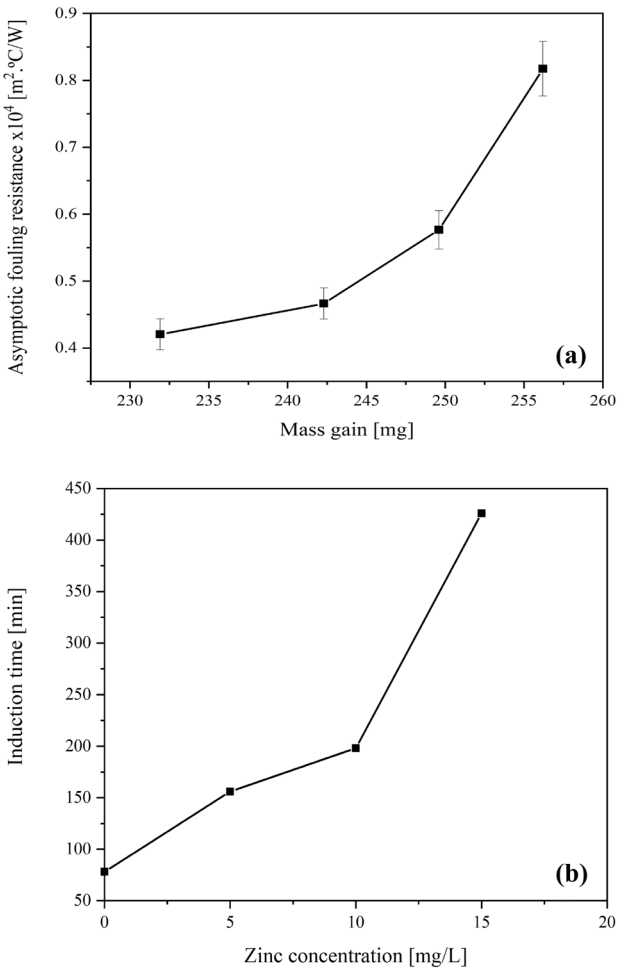

Fig. 9 (**a**) Thermal fouling resistance as a function of scale mass and (**b**) crystallisation fouling induction time for different concentrations of zinc in water

to 426 minutes when the Zn^{2+} concentration raised from 0 to 15 mg/L, as displayed in Fig. 9b. The presence of Zn^{2+} in a solution suppresses the nucleation and growth of scale particles through the complexation with the foulants [9–11, 16]. Another inhibition mechanism, the high frequency of adsorption of Zn^{2+} at the nuclei sites, may mitigate the nucleation rate [17].

On the other hand, the co-precipitation of zinc carbonate ($ZnCO_3$) and hydrozincite ($Zn_5(CO_3)_2(OH)_6$) crystals may occur at a Zn^{2+} concentration greater than 6 mg/L [5, 6, 17]. The morphology investigations show that the Zn^{2+} has changed the structure of deposits, as displayed in the SEM images in Fig. 10. In the absence of zinc, the deposits from potable water comprise loose needle-like aragonite particles. However, smooth flat islands are distributed on the flower-like aragonite when 10 mg/L is added to the test solution. At a concentration of 15 mg/L, the formed crystal structure completely changed. This morphology might have

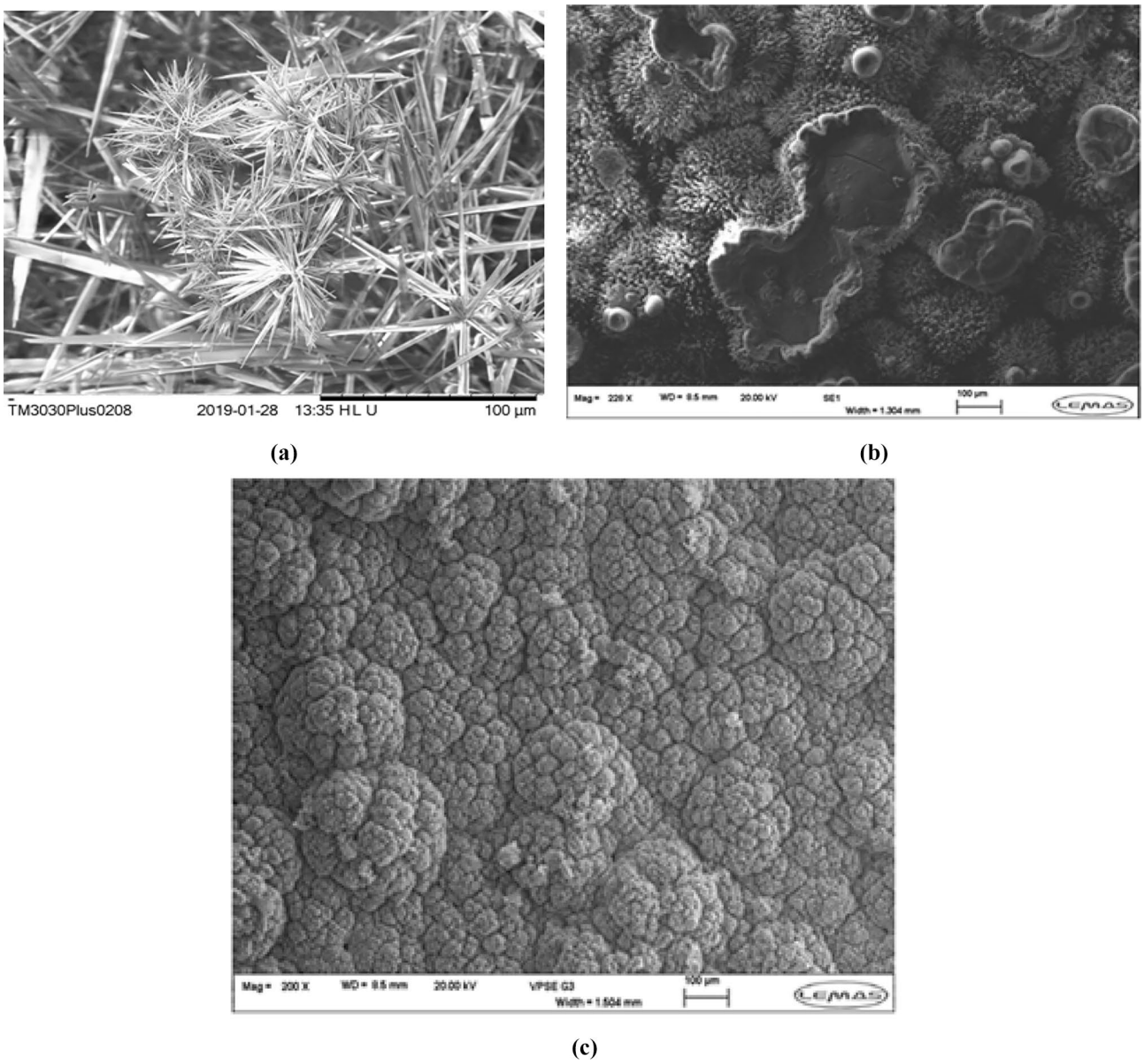

Fig. 10 SEM image for deposits on the aluminium surface for different concentrations of TOC; (**a**) no Zinc, (**b**) $[Zn^{2+}] = 10$ mg/L and (**c**) $[Zn^{2+}] = 15$ mg/L

resulted from aragonite crystal poisoning with Zn^{2+} and/or co-precipitation of zinc deposits.

Figure 11 shows the elemental analysis (EDX) of the fouling layer for the three tested concentrations. The zinc content of deposits increased from 4.54 wt% to 16.68 wt% as the Zn^{2+} concentration in the solution increased from 5 to 15 mg/L proving the interaction between Zn^{2+} and mineral scale particles. It has been emphasised by Glasner and Weiss [6] that the carbonate complex $[Zn(CO_3)_2]^{2-}$ acts as a nucleation site for $CaCO_3$ crystals. The affinity of Zn^{2+} to the carbonate ions is greater than Ca^{2+}. Therefore, the combination between Zn^{2+} and CO^{-}_3 is more likely at high concentrations of Zn^{2+} forming $[Zn(CO_3)_2]^{2-}$, $Zn_5(CO_3)_2(OH)_6$ or $ZnCO_3$ on the heat transfer surface.

4 Conclusions

In the present work, the influence of Zn ions in potable water on the kinetics of precipitation and the structure of the scale particles were investigated using a unique batch system associated with the steaming process. Moreover, the fouling rate and morphology of the fouling layer on a heated surface in a once-through flow system were examined. Using a batch

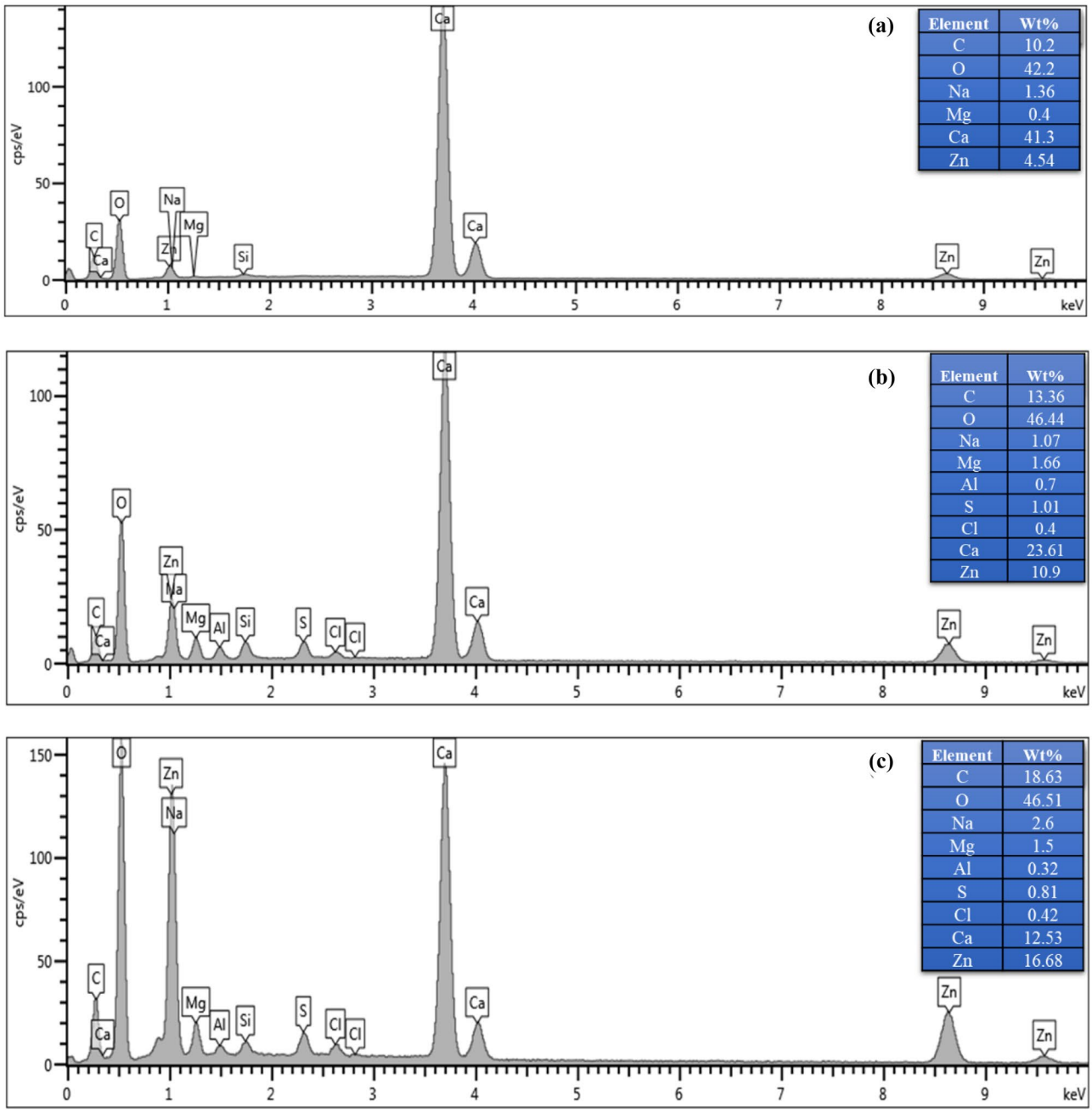

Fig. 11 EDX elemental analysis of the deposits on aluminium; (**a**) $[Zn^{2+}] = 5$ mg/L, (**b**) $[Zn^{2+}] = 10$ mg/L and (**c**) $[Zn^{2+}] = 15$ mg/L

steam generator system showed that the presence of Zn^{2+} reduces the consumption rate of Ca^{2+} during potable water heating. Furthermore, the induction time of $CaCO_3$ crystallisation was prolonged as the content of Zn^{2+} increased. Analysis of Zn^{2+} concentration as a function of time refers to Zn^{2+} consumption either in complexation with other foulants or in the crystallisation reaction to $ZaCO_3$. The presence of $ZnCO_3$ as a smithsonite was confirmed by PXRD analysis. Zn^{2+} in scaling potable water also affects the morphology of the precipitates, changing from fine needles to lumps.

The fouling resistance approach and deposit mass were used to evaluate the influence of zinc on the deposition of the inorganic minerals on the aluminium surface in the open system. The results exhibited that the fouling resistance decreases with the increase of the Zn^{2+} concentration. In terms of fouling morphology, the size of particles reduces significantly due to the impact of Zn^{2+} on the crystal growth. Moreover, the EDX findings showed that the fouling layer content of zinc increases with a solution concentration of $Zn^{2+,}$ confirming the deposition of zinc minerals.

Acknowledgements The authors acknowledge the funding and support from the Leeds University SALSAS consortium. We also wish to acknowledge the technical and administrative team of the Institute of Functional Surfaces (IFS), School of Mechanical Engineering at the University of Leeds, for their support.

References

1. Meyer H (1984) The influence of impurities on the growth rate of calcite. J Cryst Growth 66(3):639–646 (Art no)
2. Organization WH (2003) Zinc in Drinking-Water: Background Document for Development of WHO Guidelines for Drinking-Water Quality. 2003, ed
3. Coetzee P, Yacoby M, Howell S (1996) The role of zinc in magnetic and other physical water treatment methods for the prevention of scale. Water SA 22(4):319–326. https://hdl.handle.net/10520/AJA03784738_1096
4. Zachara JM, Kittrick JA, Harsh JB (1988) The mechanism of Zn2 + adsorption on calcite. Geochimica et Cosmochimica Acta 52(9):2281–2291. https://doi.org/10.1016/0016-7037(88)90130-5
5. Zeppenfeld K (2010) Prevention of $CaCO_3$ scale formation by trace amounts of copper (II) in comparison to zinc (II). Desalination 252(1–3):60–65. https://doi.org/10.1016/j.desal.2009.10.025
6. Glasner A, Weiss D (1980) The crystallisation of calcite from aqueous solutions and the role of zinc and magnesium ions—I. Precipitation of calcite in the presence of Zn2 + ions. J Inorg Nucl Chem 42(5):655–663 (Art no)
7. Al-Gailani A, Sanni O, Charpentier TVJ, Crisp R, Bruins JH, Neville A (2020) Examining the effect of ionic constituents on crystallisation fouling on heat transfer surfaces. Int J Heat Mass Transf 160:120180. https://doi.org/10.1016/j.ijheatmasstransfer.2020.120180
8. Al-Gailani A, Charpentier TV, Sanni O, Neville A (2021) Crystallisation fouling in domestic appliances and systems. Heat Transfer Eng 1–10. https://doi.org/10.1080/01457632.2021.1963091
9. Ghizellaoui S, Euvrard M, Ledion J, Chibani A (2007) Inhibition of scaling in the presence of copper and zinc by various chemical processes. Desalination 206(1–3):185–197. https://doi.org/10.1016/j.desal.2006.02.066
10. Pernot B, Euvrard M, Remy F, Simon P (1999) Influence of Zn (II) on the crystallisation of calcium carbonate application to scaling mechanisms. Aqua- Jo Water Services Res Technol 48(1):16–23
11. Ghizellaoui S, Euvrard M (2008) Assessing the effect of zinc on the crystallisation of calcium carbonate. Desalination 220(1):394–402. https://doi.org/10.1016/j.desal.2007.02.044
12. Stumm W, Morgan JJ (2012) Aquatic chemistry: chemical equilibria and rates in natural waters. John Wiley & Sons
13. Wenjun L, Hui F, Lédion J, Xingwu W (2009) Anti-scaling properties of zinc ion and copper ion in the recycling water. Ionics 15(3):337–343. https://doi.org/10.1007/s11581-008-0270-8
14. knovel (2020) Physical Constants of Inorganic Compounds, ed
15. Abouali E, Jean O, Lédion J (1996) Influence du cuivre et du zinc sur le pouvoir entartrant de l'eau. J européen d'hydrologie 27(2):109–126 (Art no)
16. Meyer HJ (1984) The influence of impurities on the growth rate of calcite. J Cryst Growth 66(3):639–646. https://doi.org/10.1016/0022-0248(84)90164-7
17. Sabzi R, Arefinia R (2019) Investigation of zinc as a scale and corrosion inhibitor of carbon steel in artificial seawater. Corros Sci 153:292–300. https://doi.org/10.1016/j.corsci.2019.03.045